2MASS EXTRAGALACTIC STUDIES:
EARLY RESULTS FROM THE PROTOTYPE CAMERA

S. E. SCHNEIDER
UMass Astronomy Program, Amherst, MA 01003 USA
J. P. HUCHRA
CfA, Harvard College, Cambridge, MA 02138 USA
AND
T. H. JARRETT AND T. J. CHESTER
IPAC, Caltech 100–22, Pasadena, CA 91125 USA

1. Introduction

The prototype camera of the Two-Micron All Sky Survey (2MASS) has now collected near-infrared data in a variety of stellar and extragalactic environments and under a range of seeing and photometric conditions. This has provided us with an opportunity to "exercise" the processing pipeline and "tune" the algorithms for identifying galaxies. We have begun to explore some of the results from the fields examined so far to better understand the survey parameters.

As an introduction to the 2MASS camera, we show observations of two well-known galaxies: M51 and M104. These were both observed in the standard 2MASS step-stare observing mode, with integrations of about 8 s. Optical CCD (300 s integration) images obtained at the McDonald observatory are also shown for comparison.

In Fig. 1 we show M104 ("the Sombrero"). The lessening importance of dust absorption is illustrated. The dark band so evident in the blue (V) band becomes weak at J and is nearly invisible at K_s, so that the galaxy appears essentially symmetric from north to south. This illustrates both why infrared surveys produce more accurate stellar fluxes of galaxies, and why from *within* the Milky Way we are able to observe close to the "zone of avoidance."

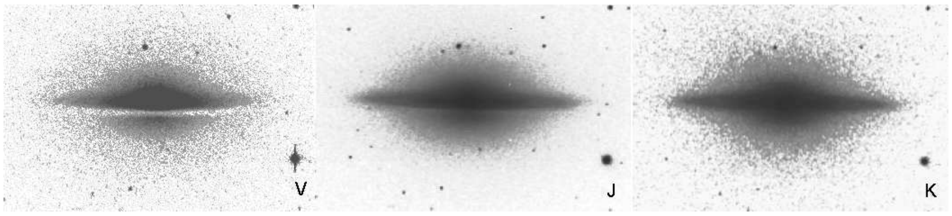

Figure 1. Images of M104 at V, J, and K_s. The J and K_s images were produced by the 2MASS prototype camera operating in standard survey mode.

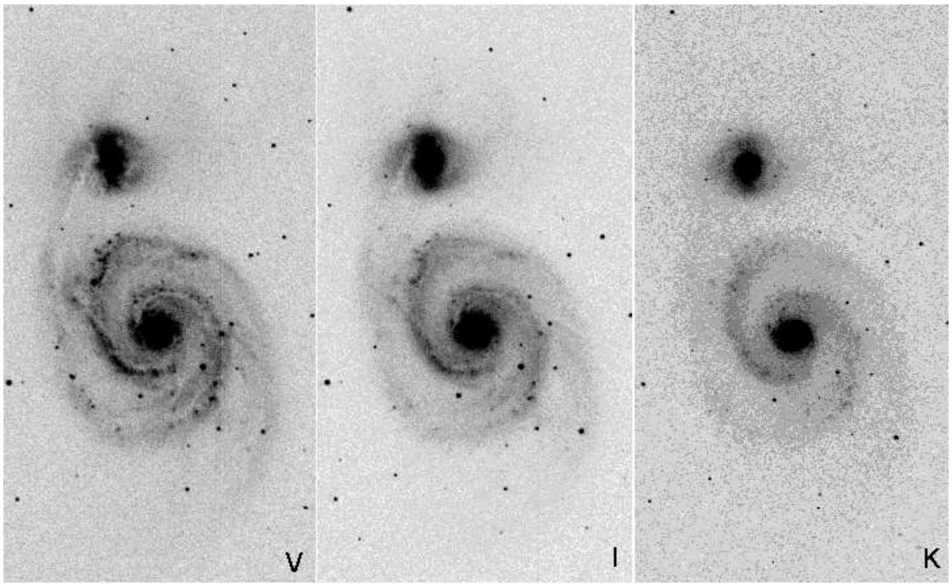

Figure 2. Images of M51 at V, I, and K_s. The K_s image was produced by the 2MASS prototype camera operating in standard survey mode.

The K_s band image of M51 ("the Whirlpool") in Fig. 2 has a much smoother structure than in the V or I band images. It is also noteworthy that low surface brightness tidal material west of the companion and the faint outer reaches of the spiral arm to the south of the galaxy are detectable in the K_s image despite the short integration time. The smoothness of the galaxy at 2μ is due partially to the lack of dust absorption, but it is also a consequence of the lower sensitivity in the infrared to the young, blue stars in star-forming regions. The infrared light better represents the underlying mass of old and low-mass stars and more clearly delineates the two-arm structure of the galaxy.

While these examples are instructive, the vast majority of galaxies cataloged by 2MASS will be much more distant and much smaller. Simply

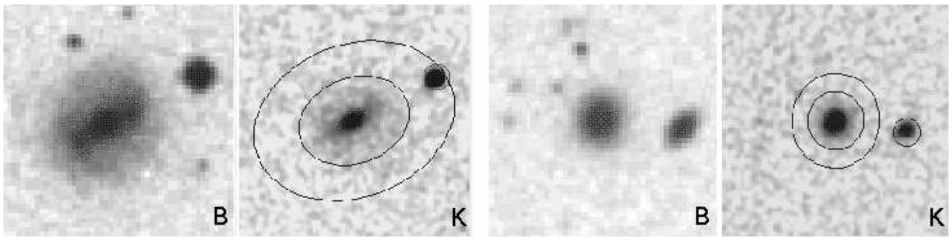

Figure 3. Optical and infrared images of a spiral (left) and an elliptical (right) galaxy. Blue-band images from the POSS and K_s band images are shown for comparison. Contours on the K_s images represent 20 and 21 mag arcsec^{-2} and the small circles identify nearby objects that were deleted by the galaxy processor in carrying out the photometry.

scaling by distance, half of the million+ galaxies in the 2MASS catalog will be within $\sim$ 25% of our minimum detectable size and within $\sim$ 0.5 mag of our magnitude limit. Identifying such galaxies in a uniform way under varying conditions is non-trivial, as we have learned with the prototype camera data. We also do not know a priori what population (e.g., depth, type, environment) these galaxies will represent, so we have begun some initial studies of galaxies identified in the prototype camera fields.

This contribution focuses on three separate topics from 2MASS' initial extragalactic studies. First, we will discuss the problem seeing presents for star/galaxy discrimination and a solution that grew out of the galaxy-identifying process. Second, we show results of redshift studies of galaxies identified in two cluster regions which indicate the range of distances of a 2MASS-identified sample. Finally, we describe the low-surface-brightness (LSB) galaxy processor that has been developed at IPAC and some of the surprising objects it is detecting.

2. Seeing and Star/Galaxy Discrimination

Galaxies more typical of what will be cataloged by 2MASS are shown in Fig. 3 along with corresponding optical images from the Palomar Observatory Sky Survey (POSS). We show the blue plate and K_s images for a spiral and an elliptical galaxy for comparison. The infrared images extend fairly clearly out to the μ_K = 20 mag arcsec^{-2} (inner elliptical contour), and the extent can be estimated to about a magnitude fainter using apertures with the same fixed axis ratio. The POSS images appear to be perhaps a magnitude deeper in surface brightness, although the different "stretches" in the images makes direct comparison difficult. On the other hand, an advantage for the infrared photometry is that the disks of spirals become bluer in the outer regions, so that a larger fraction of the total K-band light is contained within a smaller aperture.

The central galaxies in Fig. 3 are clearly extended, although a small neighbor of the elliptical is not so obviously different from the star seen next to the spiral galaxy in the K_s images. However, even a small galaxy like this spreads its light out significantly more than a star, and can be identified by a measure of the diffuseness of the light.

The 2MASS galaxy processing system was described by Chester & Jarrett (1996) at the previous DENIS conference. The star/galaxy discrimination step is carried out by fitting a generalized exponential of the form:

$$f(r) = f_0 e^{-(r/\alpha)^{1/\beta}} \tag{1}$$

to the radial distribution of pixel fluxes $f(r)$. The parameters α and β allow the distribution to take on a variety of forms ranging from Gaussian to simple exponential to a de Vaucouleurs $r^{1/4}$ law, which ought to cover the range from stars to spirals to ellipticals.

In practice, seeing blurs the distinction between classes, and spirals and ellipticals show smaller differences because the infrared emission is dominated by bulge stars in most disk galaxies. However, for objects of the same magnitude, α and β both tend to be smaller for stars and larger for galaxies. Thus a *shape parameter* defined as the product of $\alpha \times \beta$ is a good discriminant between stars and galaxies, if not between ellipticals and spirals. We use this parameter in conjunction with the more traditional central flux vs. total flux relation to distinguish galaxies and stars.

Unfortunately, the shape parameter (like other measures of diffuseness) also grows larger for all objects as the seeing grows worse. It is possible to calibrate this if the psf is well-known (except for the smallest galaxies which become indistinguishable from stars when the seeing is worse), but we must track the seeing to within $\sim 0\farcs1$. Otherwise, many galaxies near the survey limit will be mistaken for stars if the psf is overestimated, and many stars for galaxies if the psf is underestimated. It is also necessary to know the psf accurately to do accurate point source photometry, and to determine whether to accept a scan for the final survey.

This appeared to be a serious problem since such small variations in the psf significantly affected the value of the shape parameter. However, the problem provided its own solution.

Since the shape parameter is so sensitive to the seeing, we now use it to track the seeing by determining $\alpha \times \beta$ for all sources as one of the first steps in the overall "processing pipeline." Stars are so numerous, even at high Galactic latitude, that we can preferentially clip the high values of $\alpha \times \beta$ (to eliminate galaxies) and determine the mean shape parameter of the stars on very short time intervals. Fig. 4 shows two scans through the Coma cluster at high Galactic latitude under good and poor seeing conditions, and the value of the mean shape parameter for stars. Note that under the poorer

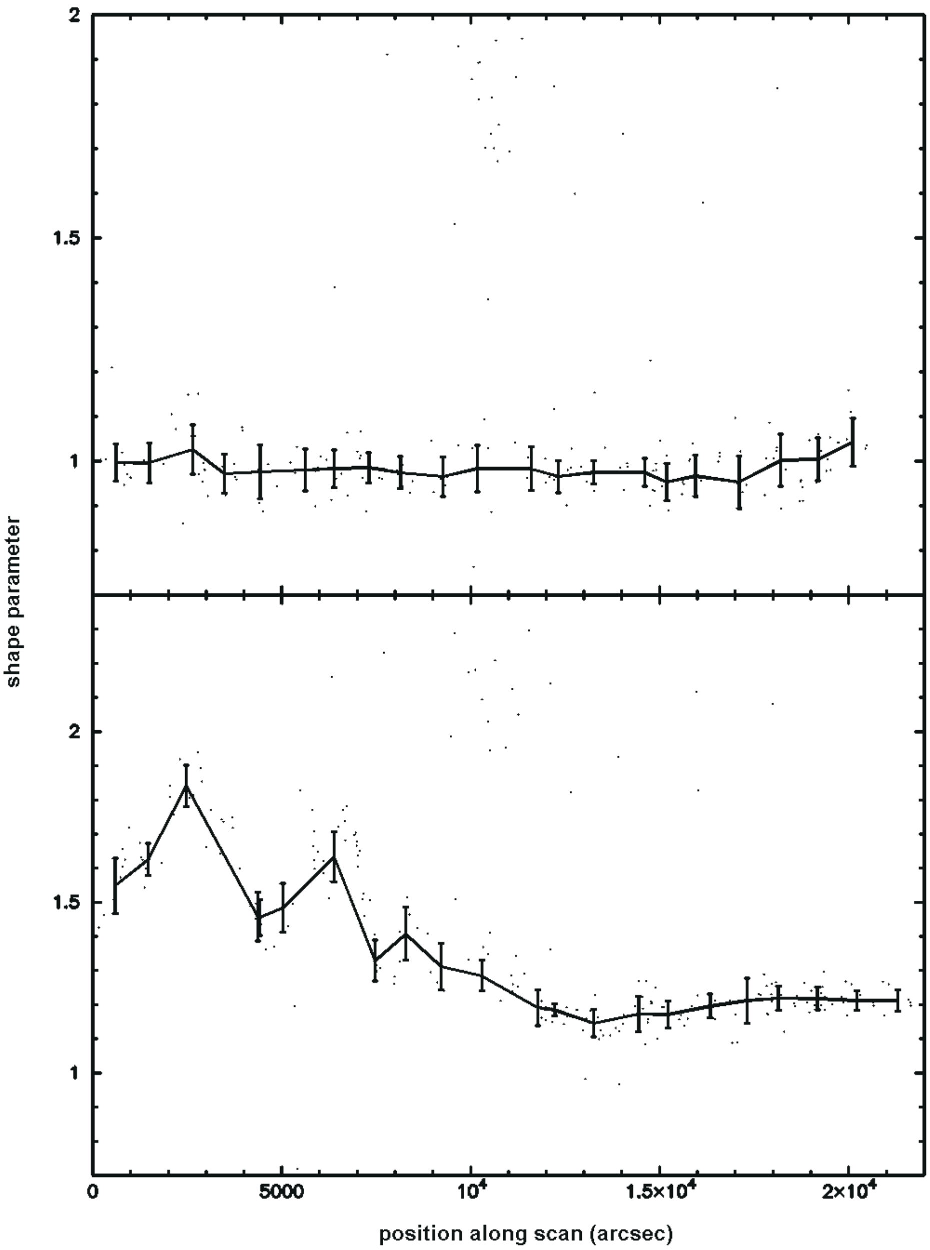

Figure 4. Values of the galaxy "shape parameter" for all sources in two scans through the Coma cluster obtained under different seeing conditions. The total duration of the scans is about six minutes. The stars have small shape parameters (around 1 under good seeing), and by measuring the mean of the low values (line through points) we can track the seeing. The full width at half maximum of the seeing- and pixel-convolved psf ranges from $\sim 2''.3$ for a shape parameter of 1.0 to $\sim 3''.7$ for a shape parameter of 1.8.

seeing conditions, not only is the seeing worse overall, it is also much more variable.

3. Redshifts of 2MASS Galaxies

We have examined the redshifts of galaxies in the vicinity of two clusters mapped by the prototype camera: $\sim 2° \times 6°$ areas toward Coma and Abell 262. We targeted cluster regions to test the galaxy processor, but it now appears likely that most of the galaxies detected are background sources!

The results for Coma are based on 266 redshifts from the literature (primarily Caldwell et al. 1993; Colless & Dunn 1996; Kent & Gunn 1982; and van Haarlem et al. 1993) for galaxies that matched one of the 628 2MASS K-band galaxy positions to within $15''$. (84% matched to within $5''$, including all of the interesting high redshift cases mentioned below.) The redshifts are better than 90% complete for galaxies with $K_s < 12$ mag, but only 30% complete for fainter magnitudes.

In every magnitude range at least 70% of the galaxies have a redshift within the range of the Coma cluster. However, it's important to keep in mind that our selection procedure gives us the peculiar bias of a K-band selected subset of an optically-determined sample. In particular, we are unlikely to have redshifts for the fainter, redder galaxies. Therefore, we cannot safely assume that the fainter galaxies in fact are as highly clustered in Coma as these statistics would suggest.

We plot absolute K magnitudes vs. redshifts in Fig. 5. The large collection of galaxies near $cz = 7000$ km s^{-1} is the Coma cluster, but note that 2MASS identified galaxies with redshifts as large as $z = 0.2$. Also note that at redshifts much larger than Coma, 2MASS is only detecting very high luminosity galaxies—each of these points may reflect an underlying cluster.

We generated the same type of plot for the Abell 262 cluster using redshifts from the literature. These data were more sparse, but looked basically similar. However, we have now obtained new redshifts that are $> 90\%$ complete down to $K_s < 13$ mag, and 50% complete between 13 and 13.5 mag. (This field was surveyed with an earlier version of the 2MASS prototype camera, and is not quite as deep as the data for Coma.) The resulting magnitude–redshift diagram for 250 of the 337 2MASS galaxies in this region is shown in Fig. 6.

This essentially K-band-selected sample not only has a few high-z members; *most* of the fainter galaxies lie at much higher redshifts than the targeted cluster. In fact, the mean redshift of the selected galaxies is 17000 km s^{-1}. If this is a typical region, and if the poorer optics of the earlier incarnation of the 2MASS protocamera has not caused some sort of strange bias, then 2MASS will identify galaxies fairly densely out to $z \sim 0.1$

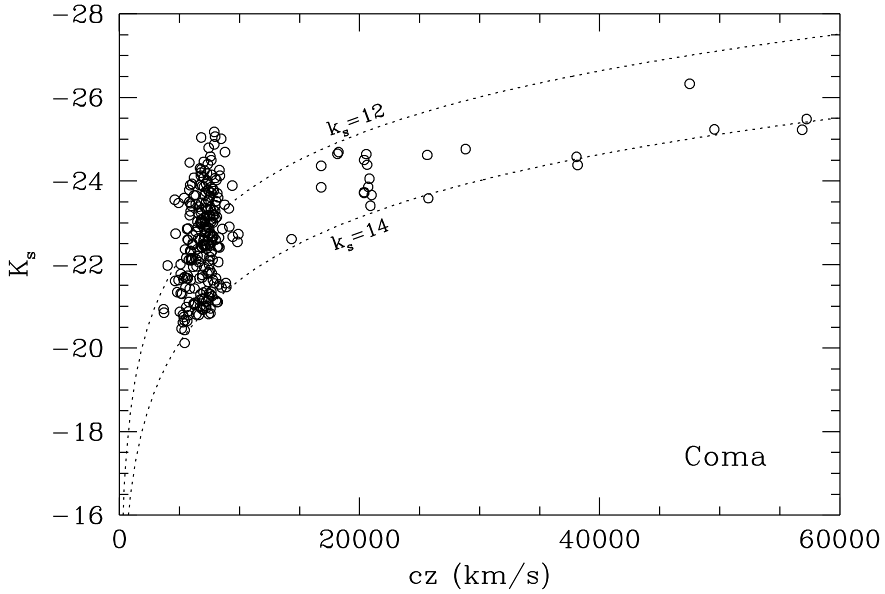

Figure 5. Absolute magnitudes vs. redshifts for galaxies in the direction of the Coma cluster ($cz \sim 7000$ km s^{-1}). The absolute magnitudes are based on the redshift and a Hubble constant of 75 km s^{-1} Mpc^{-1}. The locus of galaxies with apparent K_s magnitudes of 12 and 14 are shown by dashed lines.

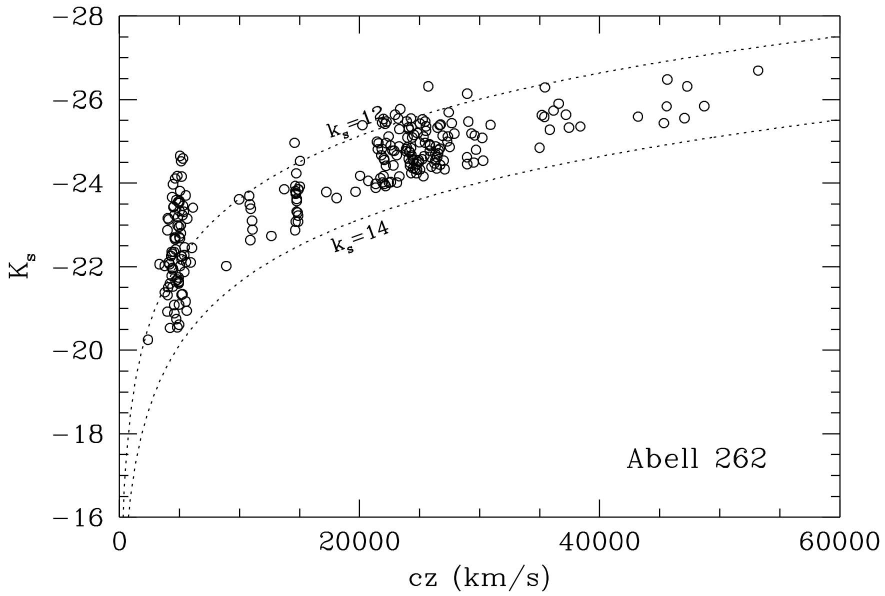

Figure 6. Absolute magnitude–redshift diagram toward the Abell 262 cluster ($cz \sim 5000$ km s^{-1}), as in the previous figure.

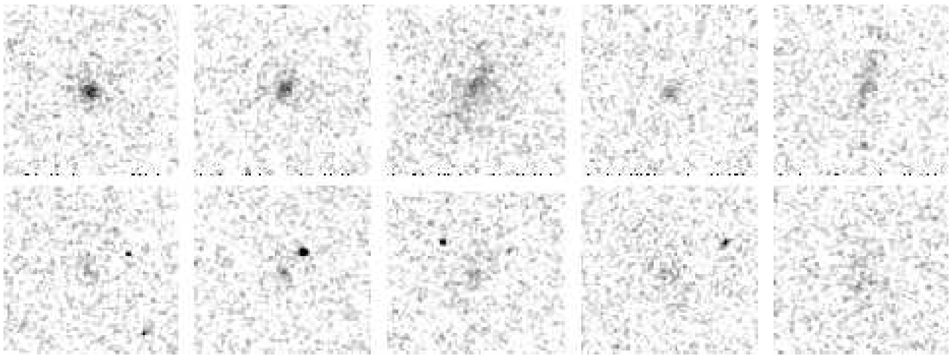

Figure 7. Examples of K_s-band objects found with the LSB galaxy processor.

4. Low Surface Brightness Galaxies

We close this introduction to 2MASS extragalactic work with some initial results from the LSB galaxy processor. This was described in principle by Chester & Jarrett at the previous meeting, but it had not been implemented at that time. The basic idea is straightforward—by averaging over many pixels, the noise can be averaged down to lower levels, and LSB galaxies can be detected.

This has now been tested using a three-step procedure: first, all previously identified stars and galaxies are cut out of the image; then the pixels are block averaged over 4×4, 8×8, and 16×16 areas, and Gaussian smoothed; finally, sources exceeding $\sim 3\times$ the background noise are selected.

This procedure depends on the uniformity of the image, which fortunately appears to be very good. Examples of the objects found are shown in Fig. 7. A number of dwarfs and other LSB galaxies identified in previous catalogs like the Virgo Cluster Catalog (Binggeli et al. 1985) have been identified, as well as some uncataloged sources that do appear to be present on the POSS. This promises to be an interesting avenue for future research.

References

Binggeli, B., Sandage, A., & Tammann, G. A. 1985, AJ, 90, 1681
Caldwell, N., Rose, J. A., Sharples, R. M., Ellis, R. S., & Boser, R. G. 1993, AJ, 106, 473
Chester, T. J., & Jarrett, T. 1995, 2nd DENIS Euroconference
Colless, M., & Dunn, A. M. 1996, ApJ, 458, 435
Kent, S. M., & Gunn, J. E. 1982, AJ, 87, 945
van Haarlem, M. P., Cayon, L., Gutierrez de la Cruz, C., & Martinez-Gonzalez, E., 1993, MNRAS, 264, 71